REVISITING SH-WAVE DATA USING LOVE-WAVE ANALYSIS

Jianghai Xia, Kansas Geological Survey, The University of Kansas, Lawrence, Kansas
Richard D. Miller, Kansas Geological Survey, The University of Kansas, Lawrence, Kansas
Recep Cakir, Washington State Department of Natural Resources, Olympia, Washington
Yinhe Luo, China University of Geosciences, Wuhan, China
Yixian Xu, China University of Geosciences, Wuhan, China
Chong Zeng, Kansas Geological Survey, The University of Kansas, Lawrence, Kansas

Abstract

Although Love waves are widely analyzed in earthquake seismology, there is much less attention on utilizing Love waves than Rayleigh waves by the near-surface community. Unlike incident P and Sv waves, a plane SH wave for a series of horizontal layers refracts and reflects only SH waves, which makes the shallow SH-wave refraction method more popular to define shear (S)-wave velocity in near-surface geologic applications. For this reason, abundant SH-wave refraction data have been acquired and S-wave velocities have been determined using their first arrivals. If signals are recorded long enough, Love-wave energy can be clearly observed on SH-wave refraction data. Wave conversion may occur in an SH-wave refraction and Love-wave analysis only results in SH-wave velocities, which suggest that we may benefit from revisiting the existing SH-refraction data using multichannel analysis of Love waves (MALW). We used numerical modeling results and real-world examples to demonstrate three advantages of revisiting SH-wave data using the MALW method. Owing to a long geophone spread commonly used in SH-wave refraction survey, a sharp image of Love-wave energy can be generated, allowing better pickings for the phase velocities of Love waves. Because Love waves are independent of P-wave velocity, “mode crossing” in an image of Love-wave energy is less common than in Rayleigh-wave images. Fewer unknowns in the method MALW make dispersion curves of Love waves are simpler, which leads to more stable inversion of Love waves and reduces the degree of nonuniqueness.

Introduction

Surface-wave techniques have been given increasingly more attention by the near-surface community with applications to a variety of near-surface problems. Studies on high-frequency surface-wave techniques have been focused primarily on Rayleigh waves. Errors in shear (S)-wave velocities obtained by inversion of Rayleigh waves (Xia et al., 1999) using a multichannel recording system (e.g., Song et al., 1989) are 15% or less and random when compared with direct borehole measurements (Xia et al., 2002a). Examples of studies on Rayleigh-wave data analysis include: near-surface quality factors (Q) (Xia et al., 2002b); a pitfall using SH-wave refraction surveying (Xia et al., 2002c); joint inversion of refractions and Rayleigh waves (Ivanov et al., 2006a); estimation of S-wave velocities for a continuous earth model (Xia et al., 2006a); the nearest offset and cutoff frequencies (Xia et al., 2006b, Xu et al., 2006, 2009); discussion of Rayleigh-wave inversion with a high-velocity-layer intrusion model (Calderón-Macías and Luke, 2007); a low-velocity-layer intrusion model (Lu et al., 2007; Liang et al., 2008); dispersive images using slant stacking (Xia et al., 2007a) and high-resolution Radon transform (Luo et al., 2008); mode separation (Luo et al., 2009), numerical modeling (Xu et al., 2007); assessment of an inverted model (Xia et al., 2008, in press); inversion of multimode data (Xia et al., 2000, 2003; Beaty et al., 2002; Luo et al., 2007); and other applications of delineation of bedrock (Miller et al., 1999) and detection of voids (Xia et al., 2004, 2007b) and shallow fault zone (Ivanov et al., 2006b).

Although Love waves are widely analyzed in earthquake seismology (e.g., Aki and Richards, 1980), for example, a simultaneous inversion of phase velocities of Love and Rayleigh waves in the study of the earth structures (Lee and Solomon, 1979), there is much less attention on utilizing Love waves than Rayleigh waves by the near-surface community (Steeples, 2005). This may be because acquiring SH-wave data is not as easy as acquiring vertical-component P-wave and Rayleigh-wave data and/or the unavailability of software for Love-wave analysis. Recent improvements in data-acquisition techniques and developing of software make SH-wave data acquisition and processing easier. In addition, analyzing SH-wave data using Love-wave inversion for near-surface applications may become more useful because it provides SH-wave velocities that are critical for S-wave and anisotropy analysis.

Recent studies on high-frequency Love waves include sensitivity analysis (Zeng et al., 2007); improvement of S-wave velocity with Love-wave inversion (Safani et al., 2005), inversion of Love waves with a low-velocity layer (Safani et al., 2006), joint inversion of electric and Rayleigh- and Love-wave data (Misiek et al., 1997), and inversion of Love-wave data to measure the lateral variability of geo-acoustic properties of marine sediments (Winsborrow et al., 2003). High-frequency Love-wave modeling by Luo et al. (in review) could improve the inversion of Love waves in the time-space domain. Sharp dispersion images and stable inversion of Love-wave data with the weighted least-square method provided reliable S-wave velocities in several sites (Xia et al., 2009). Wave conversion may occur in an SH-wave refraction survey (Xia et al., 2002c) and Love-wave analysis only results in SH-wave velocities, which suggest that we may benefit from a revisit to existing SH-refraction data to use Love waves for determining S-wave velocities using multichannel analysis of Love waves (MALW).

Love waves are the result of total internal multiple reflections of SH waves at the free surface. Their particle motion is parallel to the surface but perpendicular to the direction of propagation. For a layered-earth model, the condition for existence of Love waves is the same as the condition for existence of refractions (e.g., Stoneley, 1950; Garland, 1979). Based on their field experiences, Eslick et al. (2008) concluded that a minimum thickness of 1 m of low-velocity material for the near-surface layer is needed to record usable Love-wave data in the frequency range of interest (5-50 Hz). Love-wave phase velocity of a layered-earth model is a function of frequency and three layer parameters: SH-wave velocity, density, and thickness of layer. The dispersion of Love waves is independent of P-wave velocity (Aki and Richards, 1980). This property is extremely useful in inversion of Love waves for S-wave velocities and reduces the degree of nonuniqueness of an inverted S-wave velocity model. In addition, Love waves in a layered-earth model also possess the unique properties that the asymptote of the phase and group velocities at high frequencies approaches the S-wave velocity of the top layer and the asymptote at low frequencies approaches the S-wave velocity of the half space. Xia et al. (2009) generally discussed an inversion algorithm of the MALW method and showed their dispersion analysis and inversion results of SH refraction data acquired at various sites in the US. Although the data were acquired for SH-refraction analysis focused on first breaks and recorded with a short time length (Love waves were not completely recorded), dispersion analysis of these data show that Love-wave energy can be sharply and clearly imaged and phase velocities then are easily determined. The inversion of these phase velocities was very stable and extremely fast.

In this paper, we will use numerical modeling results and real-world examples to demonstrate the three advantages of the MALW by revisiting SH-wave data with Love-wave analysis in defining S-wave velocity. Owing to a long geophone spread commonly used in SH-wave refraction survey, an image of Love-wave energy is cleaner and sharper than Rayleigh waves, which makes picking phase velocities of Love waves much easier and more accurate. Because it is independent of P-wave velocity, dispersion curves of Love waves are simpler than Rayleigh waves. “Mode crossing” is an annoying phenomenon in Rayleigh-wave analysis that causes mode misidentification and therefore produces S-wave velocities much higher than real ones (Zhang and Chan, 2003). “Mode crossing,” however, is less common in

dispersion images of Love-wave energy than Rayleigh waves. This simplicity of Love-wave dispersion curves leads to the inversion of Love waves much easier and more stable compared to Rayleigh waves.

Sharp Images of Dispersive Energy of Love Waves

Resolution (or sharpness of a trend of energy peaks) of a dispersive image is approximately proportional to a geophone spread, which is a distance between the first geophone to the last geophone (Forbriger, 2003; Xia et al., 2006b). SH-wave refraction surveying usually uses a long geophone spread. An image of dispersive energy generated from the SH-wave refraction data is normally sharp enough to ensure that the picked phase velocities are accurate in general, which provides a solid basis for reprocessing SH-wave refraction data using Love-wave analysis.

SH-wave refraction data of the first example was acquired in Wyoming during the fall of 1998 to determine shear-wave velocities in near-surface materials (upper 7 m). SH-wave refraction data were acquired using 48 28-Hz horizontal-component geophones oriented in a N-S direction. Geophones were deployed at a 0.9-m interval along a W-E line. A polarized seismic source was provided by a 6.3-kg hammer impacting the long dimension of a fixture (S-wave source plate) oriented perpendicular to the west-to-east geophone spread. Two records were generated for each source location, one with a blow from the south and the other from the north, with a phase difference of 180^o (Figure 1). Analysis of the SH-wave refraction data using first arrivals (direct and refracted waves) produced a velocity model that was very close to a P-wave velocity model except for the first layer (Xia et al., 2002c). Processing P-wave refraction data using Rayleigh-wave analysis showed the velocity model generated from SH-wave refraction data was converted P-wave velocities on a dipping interface, which was supported by the suspension logging data (Xia et al., 2002c).

We reprocessed the SH-wave refraction data using Love-wave analysis. Strong Love-wave energy can be observed in Figure 1. Sharp images (Figure 2) from both shots were generated using the high-resolution linear Radon transform (Luo et al., 2008). Phase velocities of the fundamental mode from 10 to 50 Hz and the first higher mode from 35 to 55 Hz can be easily picked out from either one of the images, which are visually identical. We will show the inversion results later in this paper.

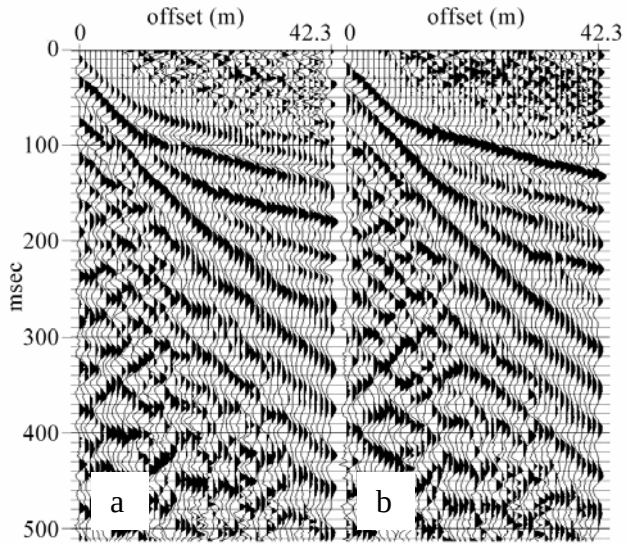

Figure 1. Forty-eight-channel SH-wave refraction data along a W-E line. N-S blows against both ends of the fixture generated data with the polarity revision of the first arrivals (a and b).

SH-wave data (Figure 3a) of the second example were acquired at the front grassy area of the Kansas Geological Survey building in the spring of 2009, where Rayleigh wave data were collected along the same line in 1995 (Xia et al., 1999). The data were acquired using 40 14-Hz horizontal component geophones oriented perpendicular to the line. Geophones were deployed at a 1-m interval, and the same hammer source and SH-wave generation procedure as described in the first example were used. Figure 3a shows the shot gather (three far offset traces were removed due to noises) with strong Love waves. A sharp image (Figure 3b) from the shot gather was generated. Phase velocities of the fundamental mode from 12 to 50 Hz and first higher mode from 38 to 55 Hz can be easily picked out from the image. We will show the inversion results later in this paper.

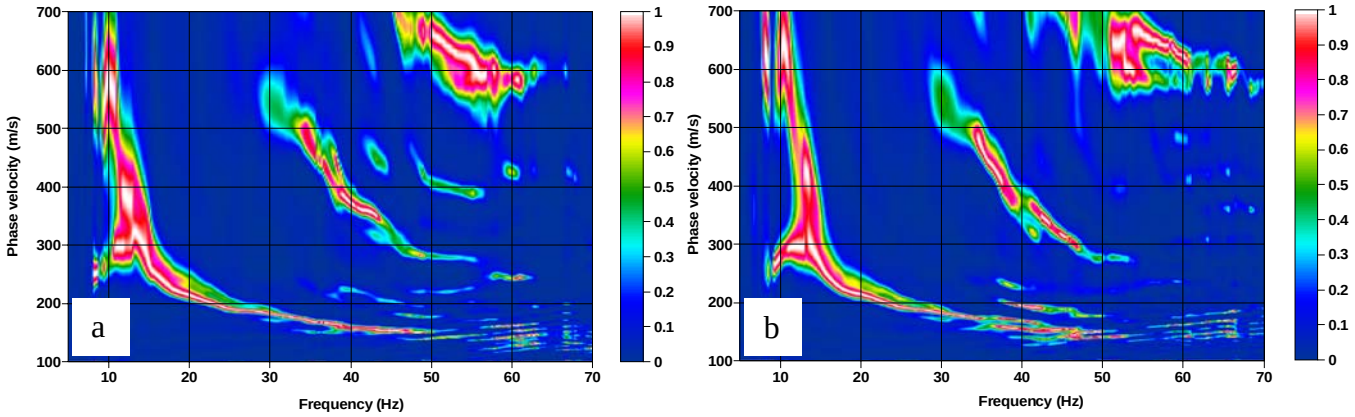

Figure 2. Images of Love-wave energy shown in Figure 1. (a) generated from the shot gather shown in Figure 1a from a blow from the south and (b) generated from the shot gather shown in Figure 1b from a blow from the north.

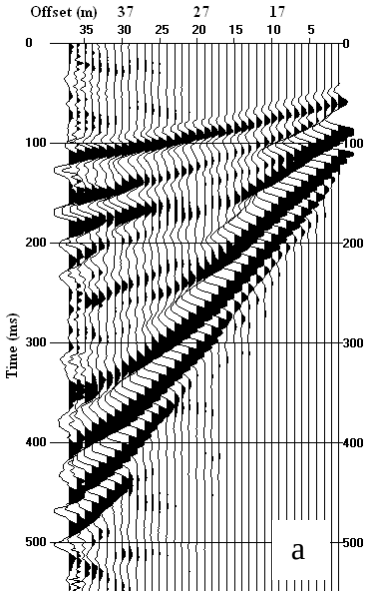

Figure 3. SH-wave data with well developed Love waves acquired in the front grassy area of the KGS building (a). An image (b) of Love-wave energy was generated using high-resolution linear Radon transform (Luo et al., 2008). The sharp Love-wave energy trend allows easy and accurate picking for phase velocities.

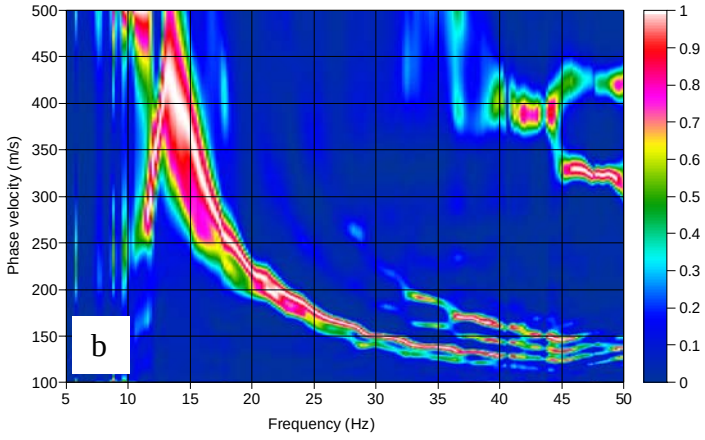

Finally, SH-wave data of the third example were acquired in Yuma, Arizona in the summer of 2009 to build a near-surface velocity model. A long-geophone-spread shot gather was used. The data were acquired using 240 14-Hz horizontal component geophones oriented perpendicular to the line. Geophones were deployed at a 1.2-m interval, and the same seismic source and procedure of SH-wave generation as described for the first example were used. Strong Love waves were present (Figure 4a). Just for a test, we kept all 240 traces for Love-wave processing. An image (Figure 4b) generated from the shot gather was sharp even though the signal-to-noise ratio was relatively low in the far offset traces (trace 170 and farther). Phase velocities of the fundamental mode from 5 to 95 Hz can be easily identified from the image, which are averaged values of the area covered by the geophone spread. To investigate the lateral velocity change, we also generated the dispersive image (Figure 4c) based on the first 50 traces. Comparing Figure 4b with Figure 4c, the phase velocities due to the shallower part of the subsurface (30 to 95 Hz) were identical but the velocities of the deeper part (5 to 30 Hz) were different, indicating lateral changes in S-wave velocity. We also noticed that longer wavelength components (> 40 m) were not well imaged in Figure 4c due to a short geophone spread.

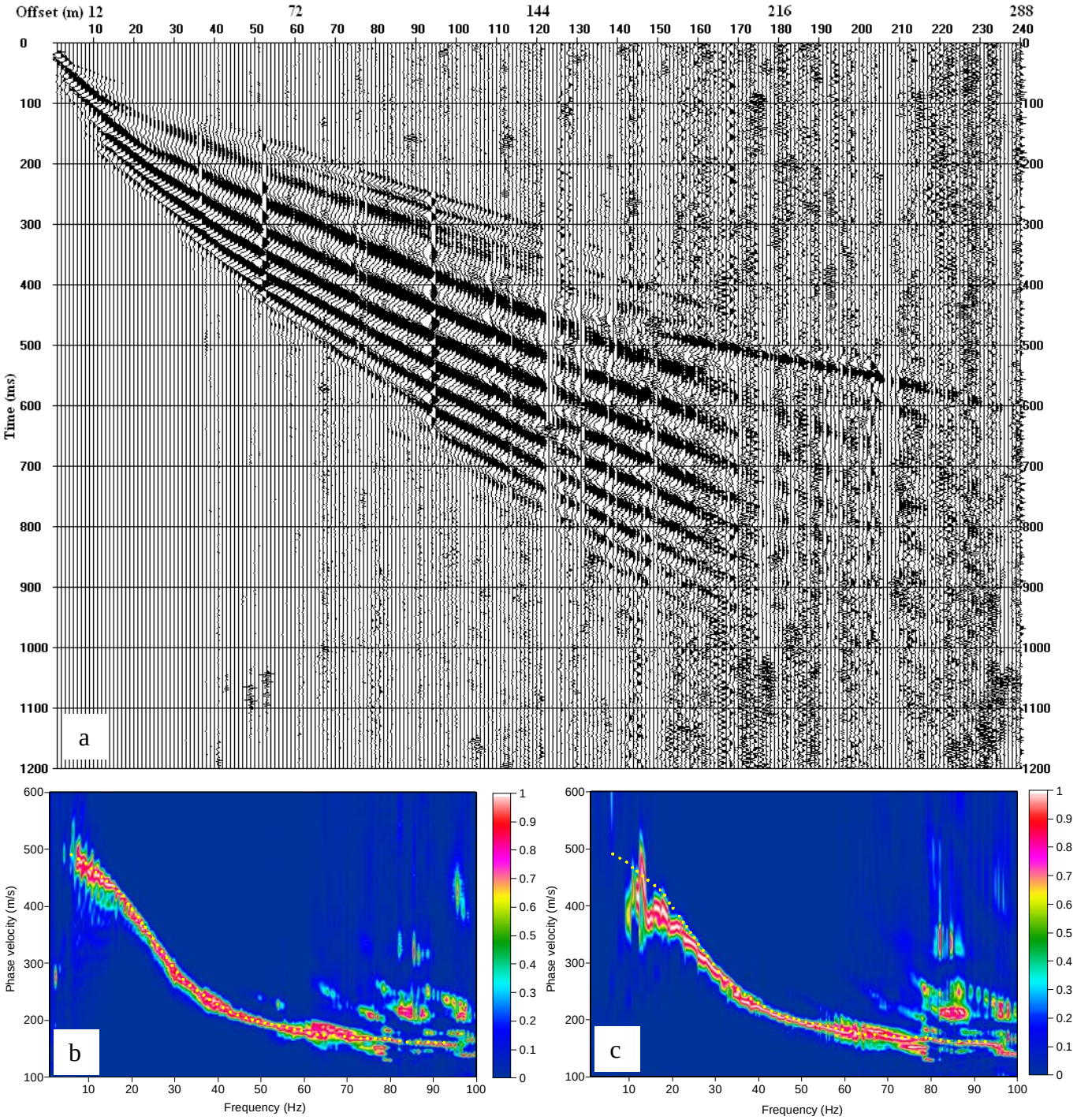

Figure 4. (a) SH-wave data with 240 traces acquired in Yuma, Arizona. Love-wave energy is dominant in the shot gather. (b) An image of Love-wave energy calculated from the 240-trace shot gather (a) containing noisy traces. The sharp Love-wave energy trend allows easy and accurate pickings of phase velocities (yellow dots). (c) An image of Love-wave energy was calculated from the first 50 traces of the shot gather (a) superposed with yellow dots that are phase velocities picked from (b). Note that phase velocities are the same from 30 Hz and up for both images, and phase velocities from 5 to 30 Hz are higher in (b) than in (c).

Simple Dispersion Curves of Love Waves

Unlike Rayleigh waves, the dispersion of Love waves is independent of P-wave velocity. Love-wave phase velocity of a layered-earth model is a function of frequency and three parameters: SH-wave velocity, density, and thickness of layers. A fewer parameters make the dispersion curves (or Love-wave energy trend) simpler.

We used a two-layer model, with the first layer Vs, Vp, density, and thickness as 150 m/s, 300 m/s, 1.5 g/cm^3, and 10 m, respectively, and the half space Vs, Vp, and density as 450 m/s, 900 m/s and 2.0 g/cm^3, respectively, to compare dispersion behaviors of Rayleigh and Love waves. This model simulates the case of a soft layer overlying bedrock. Figure 5a shows synthetic P-Sv data with 110 traces based on the two-layer model generated by Xu et al.'s algorithm (2007). Rayleigh waves are observed in the shot gather. Rayleigh-wave energy was mapped by the high-resolution linear Radon transform (Luo et al., 2008) in the frequency-velocity (f-v) domain (Figure 5b). It is interesting to point out that the fundamental mode may be picked from 4 to 50 Hz continuously and "confidently" if no other information is available on the subsurface, such as an S-wave velocity range. After we superposed the theoretical dispersion curves onto the image (Figure 5c), we found that at 6 Hz the fundamental mode is 313 m/s and the first higher mode 326 m/s. At current resolution of dispersive images, it is very difficult to tell that the modes have gone up at 6 Hz with this small difference, which we called "mode crossing." With some low-resolution techniques to generate an image of dispersive energy, the "mode crossing" between the second and third higher modes may also occur around 21 Hz. Previous studies (Figures 8 and 10, Xia et al., 2006b) showed that the "mode crossing" also occurs in multi-layer models in which Vs increases gradually with

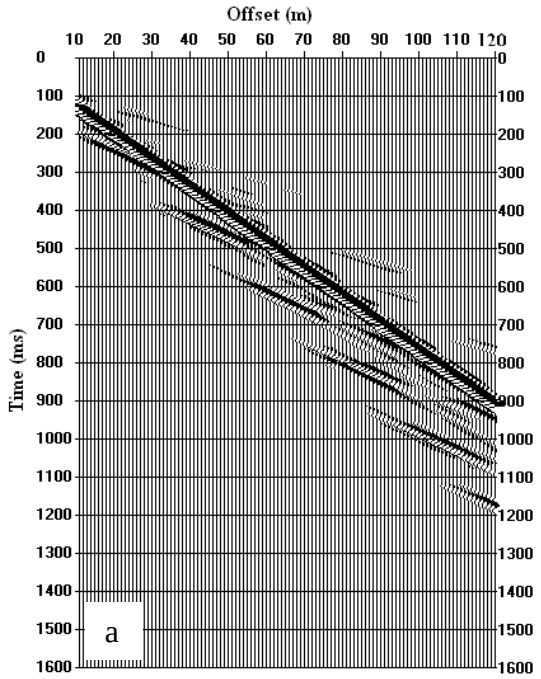

Figure 5. (a) A synthetic shot gather of P-Sv data used in Rayleigh-wave analysis.

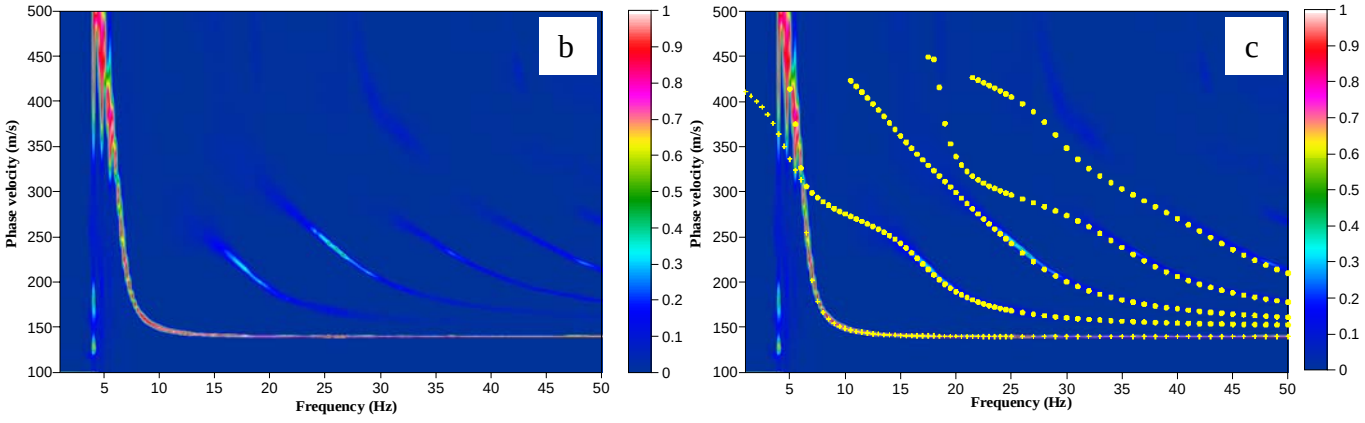

Figure 5. (b) An image of Rayleigh-wave energy calculated from the 110-trace shot gather (a). The energy of the fundamental mode appears continuously from 4 to 50 Hz. (c) Plus symbols and yellow dots, which are calculated by the Knopoff method (Schwab and Knopoff, 1972), are the fundamental and higher modes, respectively, and superposed onto (b). "Mode crossing" occurs at 6 Hz.

depth. The "mode crossing" causes mode misidentification (Zhang and Chan, 2003) that results in inverted S- wave velocities higher than true velocities.

We then modeled the SH-wave data (Figure 6a) based on the two-layer model described in the last paragraph (Luo et al., in review). The fundamental and higher modes are separated clearly (Figure 6b). The Love-wave energy trends accurately show phase velocities of different modes. The cutoff frequencies for this model can be calculated and are around n×8 Hz for the nth higher mode (Aki and Richards, 1980), where n is the order of higher modes. The asymptotes of all modes at the high-frequency end approach 150 m/s, which is the S-wave velocity of the first layer, and at the low-frequency end approach 450 m/s, which is the S-wave velocity of the half space. The "mode crossing" does not occur in the image of Love waves for this soft-layer model (Figure 6b) nor for the multi-layer models showed by Xia et al. (2006b). The "mode crossing" may occur between the second and third higher modes for a high-velocity layer model (Luo et al., in review). It is not common to observe the second and third higher modes in real data, so the "mode crossing" is rare in real Love-wave data.

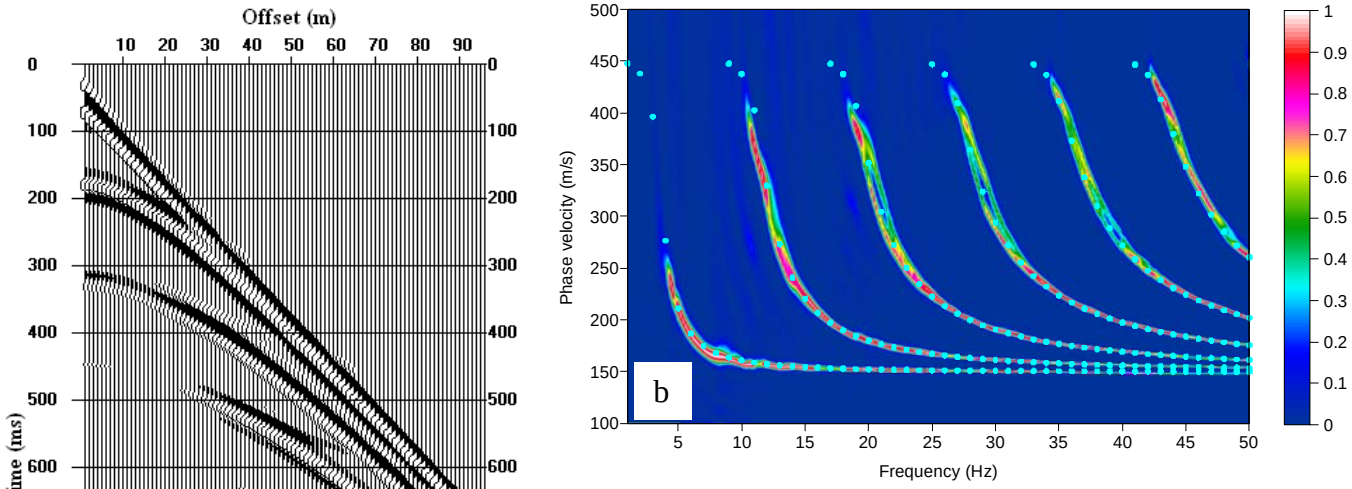

Figure 6. (a) Synthetic SH-wave data based on the two-layer model described in the text. (b) An image of Love-wave energy calculated from (a) with superposed cyan dots that are analytical results calculated by the Knopoff method (Schwab and Knopoff, 1972).

Stable Inversion of Love Waves

Inversion of phase velocities of Love waves was developed based on the algorithm discussed by Xia et al. (1999). Detailed description of the inversion algorithm can be found in Xia et al. (2009). As pointed out in the last section and based on the real-world examples demonstrated, fewer parameters make inversion of Love waves more stable.

We first inverted the data shown in Figures 1 and 2. Initial S-wave velocities were determined based on values of asymptotes at the high- and low-frequency ends for the S-wave velocities of the first layer and the half space and values of interpolations between the asymptotes for initial S-wave velocities of the layers between the first layer and the half space. We used the same thickness model as used in Rayleigh waves (Xia et al., 2002c). Two data sets of phase velocities shown by cyan dots (Figure 7a) were inverted. The first set, containing 39 fundamental phase velocities from 11 to 50 Hz, was picked by

following the energy trend in Figure 2a (the phase velocities picked from Figure 2b give the same values as those picked from Figure 2a). The second set contains the 39 fundamental phase velocities and 19 first higher mode phase velocities from 38 to 54 Hz that are also picked from Figure 2a. Inversion of either data set reached final S-wave velocity models went only in two iterations. Figure 7b shows phase velocities (Measured) picked from the image (cyan dots in Figure 7a), calculated from the initial model (Initial), and calculated from the final inverted S-wave velocity model (Final). Figure 7c shows the initial model, a final model by inversion of the fundamental data, and a final model by inversion of the fundamental and the first higher mode data simultaneously. The both inversion results are much closer to well-log results (Figure 7d), especially for the shallower part, than the SH-wave refraction results. The SH-wave refraction results, however, are converted P-wave velocities (Xia et al., 2002c).

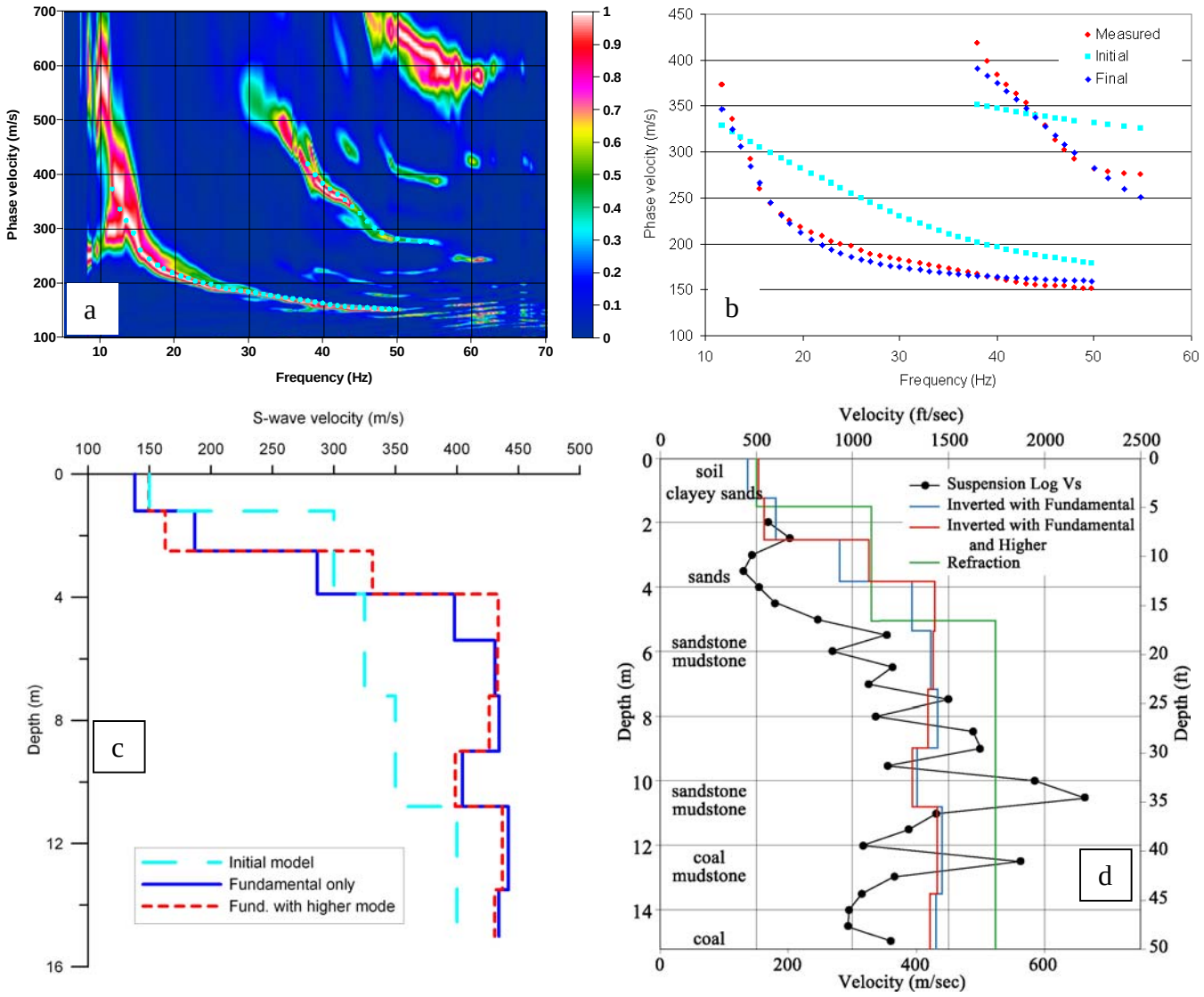

Figure 7. (a) The image of Love-wave energy (Figure 2a) superposed with picked phase velocities shown by cyan dots. (b) Phase velocities labeled “Measured” are picked from (a); those labeled “Initial” are calculated based on the initial S-wave velocity model; and those labeled “Final” are calculated based on the inverted S-wave velocity model. (c) S-wave velocity models: the initial model and inverted models from the fundamental data only and from the fundamental and the first higher mode data simultaneously. (d) Comparison among S-wave velocity models from inversion of Love waves, SH-wave refraction (a three-layer model), and the well log.

The S-wave velocity of the first layer of the final model by inversion of the fundamental and the first higher mode data simultaneously (Figure 7c) is almost the same as the asymptotic value of the fundamental phase velocities at the high frequencies (Figure 7a), while the S-wave velocity of the same layer by inversion of the fundamental data (Figure 7c) is 25% lower than the true value. This result showed that inversion of the fundamental and the higher mode data simultaneously could provide more accurate results than the fundamental data alone.

SH-wave data acquired at the front grassy area of the Kansas Geological Survey building were inverted and shown as our second example of inversion. We picked the phase velocities from the Love-wave image from 12 to 45 Hz (Figure 3b) as showed them in Figure 8a (cyan dots). We also selected a seven-layer model, the same one used in Xia et al. (1999), and arbitrarily constructed their initial S-wave velocity model. The phase velocities calculated from the initial model were far from the picked phase velocities (Figure 8b). After five iterations, the root-mean-squares error was reduced from 280 m/s to 5 m/s. The final inverted S-wave velocity model is shown in Figure 8c and compared to the borehole S-wave velocity measurements.

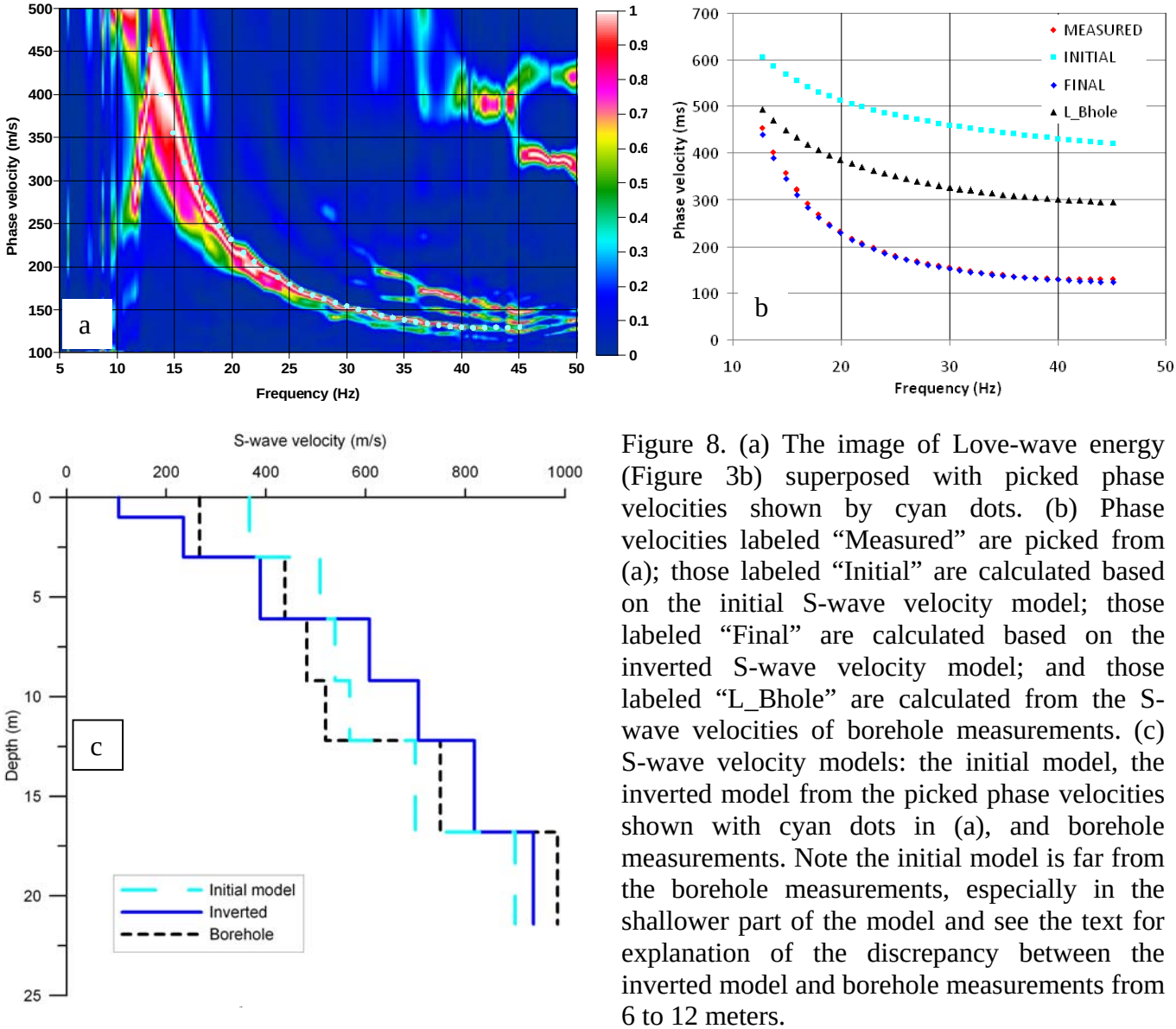

Figure 8. (a) The image of Love-wave energy (Figure 3b) superposed with picked phase velocities shown by cyan dots. (b) Phase velocities labeled “Measured” are picked from (a); those labeled “Initial” are calculated based on the initial S-wave velocity model; those labeled “Final” are calculated based on the inverted S-wave velocity model; and those labeled “L_Bhole” are calculated from the S-wave velocities of borehole measurements. (c) S-wave velocity models: the initial model, the inverted model from the picked phase velocities shown with cyan dots in (a), and borehole measurements. Note the initial model is far from the borehole measurements, especially in the shallower part of the model and see the text for explanation of the discrepancy between the inverted model and borehole measurements from 6 to 12 meters.

We noted that there are relative large differences between inverted results and borehole measurements from 6 to 12 meters (Figure 8c). To find causes of the difference, we calculated phase velocities due to borehole measurements. We found that the phase velocities due to the borehole measurements are in the middle of the phase velocities calculated from the initial model and the inverted model at each frequency (Figure 8b). This discrepancy indicates that borehole measurements provide a different S-wave velocity model and S-wave velocity anisotropy exists in this site.

Conclusions

We demonstrated and discussed three advantages of revisiting SH-wave data using the MALW method in defining S-wave velocity with synthetic and real-world data. 1) Owing to a long geophone spread commonly used in SH-wave refraction survey, images of Love-wave energy are usually cleaner and sharper than those generated from Rayleigh waves that are normally acquired using a relatively short geophone spread, which makes picking phase velocities of Love waves much easier and more accurate. 2) Because they are independent of P-wave velocity, dispersion curves of Love waves are simpler than Rayleigh waves. “Mode crossing” is an undesired phenomenon in Rayleigh-wave analysis that causes mode misidentification, which results in inverted S-wave velocities are much higher than real ones. Fortunately, this phenomenon is less common in images of Love-wave energy than Rayleigh waves. 3) Real-world examples showed that inversion of Love waves is much easier and more stable compared to Rayleigh waves, because of being independent of P-wave velocity and the simplicity of Love-wave dispersion curves. One real-world example also demonstrated that inversion of the fundamental and the first higher mode data simultaneously can provide more accurate results than the fundamental data alone. Abundant SH-wave refraction data containing non-utilized strong Love-wave energy have been acquired for various environmental and engineering applications. Our experimental study clearly shows that: 1) revisiting old SH-wave data containing Love waves can significantly contribute to detailed knowledge of existing S-wave velocity, and 2) considering Love-waves (by increasing the record length) during the future SH-wave refraction surveys can provide accurate near-surface S-wave velocities without additional cost in field.

Acknowledgments

The authors thank Marla Adkins-Heljeson of the Kansas Geological Survey for editing the manuscript.

References

Aki, K., and Richards, P.G., 1980, Quantitative seismology: W.H. Freeman and Company, San Francisco.

Beaty, K.S., Schmitt, D.R., and Sacchi, M., 2002, Simulated annealing inversion of multimode Rayleigh wave dispersion curves for geological structure: Geophys. J. Int., 151, 622–631.

Calderón-Macías, C., and Luke, B., 2007, Addressing nonuniqueness in inversion of Rayleigh-wave data for shallow profiles containing stiff layers: Geophysics, 72(1), U1-U10.

Eslick, R., Tsoflias, G., and Steeples, D.W., 2008, Field investigation of Love waves in near-surface seismology: Geophysics, 73(3), G1-G6.

Forbriger, T., 2003, Inversion of shallow-seismic wavefields: I. Wavefield transformation: Geophys. J. Int., 153, 720-734.

Garland, G.D., 1979, Introduction to geophysics: Mantle, core and crust (2nd ed.): Saunders, Toronto.

Ivanov, J., Miller, R.D., Xia, J., Steeples, D.W., and Park, C.B., 2006a, Joint analysis of refractions with surface waves: An inverse solution to the refraction-traveltime problem: Geophysics, 71(6), R131-R138.

Ivanov, J, Miller, R.D., Lacombe, P., Johnson, C.D., and Lane, J.W., Jr., 2006b, Delineating a shallow fault zone and dipping bedrock strata using multichannal analysis of surface waves with a land streamer: Geophysics, 71(5), A39-A42.

Lee, W.B., and Solomon, S.C., 1979, Simultaneous inversion of surface-wave phase velocity and attenuation: Rayleigh and Love waves over continental and oceanic paths: Bulletin of the Seismological Society of America, 69(1), 65-96.

Liang, Q., Chen, C., Zeng, C., Luo, Y., and Xu, Y., 2008, Inversion stability analysis of multimode Rayleigh-wave dispersion curves using low-velocity-layer models: Near Surface Geophysics, 6(3), 157–165.

Lu, L., Wang, C., and Zhang, B., 2007, Inversion of multimode Rayleigh waves in the presence of a low-velocity layer: Numerical and laboratory study: Geophys. J. Int., 168, 1235–1246.

Luo, Y., Xia, J., Liu, J., Liu, Q., and Xu, S., 2007, Joint inversion of high-frequency surface waves with fundamental and higher modes: Journal of Applied Geophysics, 62(4), 375-384.

Luo, Y., Xia, J., Miller, R.D., Xu, Y., Liu, J., and Liu, Q., 2008, Rayleigh-wave dispersive energy imaging by high-resolution linear Radon transform: Pure and Applied Geophysics, 165(5), 903-922.

Luo, Y., Xia, J., Miller, R.D., Xu, Y., Liu, J., and Liu, Q., 2009, Rayleigh-wave mode separation by high-resolution linear Radon transform: Geophys. J. Int., 179(1), 254-264.

Luo, Y., Xia, J., Xu, Y., Zeng, C., and Liu, J., in review, Finite-difference modeling and dispersion analysis of high-frequency Love waves for near-surface applications: Pure and Applied Geophysics.

Miller, R.D., Xia, J., Park, C.B., and Ivanov, J., 1999, Multichannel analysis of surface waves to map bedrock: The Leading Edge, 18, 1392-1396.

Misiek, R., Liebig, A., Gyulai, A., Ormos, T., Dobroka, M., and Dresen, L., 1997, A joint inversion algorithm to process geoelectric and surface wave seismic data, Part II: Application: Geophysical Prospecting, 45, 65-85.

Safani, J., O'Neill, A., Matsuoka, T., and Sanada, Y., 2005, Applications of Love wave dispersion for improved shear-wave velocity imaging: Journal of Environmental and Engineering Geophysics, 10(2), 135-150.

Safani, J., O'Neill, A., and Matsuoka, T., 2006, Love wave modelling and inversion for low velocity layer cases: Proceedings of the Symposium on the Application of Geophysics to Engineering and Environmental Problems (SAGEEP), Annual Meeting of the Environmental and Engineering Geophysical Society (EEGS), April 2-6, 2006, Seattle, WA, 1181-1190.

Schwab, F.A., and Knopoff, L., 1972, Fast surface wave and free mode computations; *in* Methods in Computational Physics, edited by B. A. Bolt: Academic Press, New York, 87-180.

Song, Y.Y., Castagna, J.P., Black, R.A., and Knapp, R.W., 1989, Sensitivity of near-surface shear-wave velocity determination from Rayleigh and Love waves: Technical Program with Biographies, SEG, 59th Annual Meeting, Dallas, Texas, 509-512.

Steeples, D.W., 2005, Near-surface geophysics: 75 years of progress: Supplement to The Leading Edge, 24 (s1), S82-S85.

Stoneley, R., 1950, The effect of a low-velocity internal stratum on surface elastic waves: Monthly Notices Royal Astronomical Society (Geophys. Suppl.), 6, 28-35.

Winsborrow, G., Huwsa, D.G., and Muyzert, E., 2003, Acquisition and inversion of Love wave data to measure the lateral variability of geo-acoustic properties of marine sediments: Journal of Applied Geophysics, 54, 71-84.

Xia, J., Miller, R.D., and Park, C.B., 1999, Estimation of near-surface shear-wave velocity by inversion of Rayleigh wave: Geophysics, 64(3), 691-700.

Xia, J., Miller, R.D., and Park, C.B., 2000, Advantage of calculating shear-wave velocity from surface waves with higher modes: Technical Program with Biographies, SEG, 70th Annual Meeting, Calgary, Canada, 1295-1298.

Xia, J., Miller, R.D., Park, C.B., Hunter, J.A., Harris, J.B., and Ivanov, J., 2002a, Comparing shear-wave velocity profiles from multichannel analysis of surface wave with borehole measurements: Soil Dynamics and Earthquake Engineering, 22(3), 181-190.

Xia, J., Miller, R.D., Park, C.B., and Tian, G., 2002b, Determining *Q* of near-surface materials from Rayleigh waves: Journal of Applied Geophysics, 51(2-4), 121-129.

Xia, J., Miller, R.D., Park, C.B., Wightman, E., and Nigbor, R., 2002c, A pitfall in shallow shear-wave refraction surveying: Journal of Applied Geophysics, 51(1), 1-9.

Xia, J., Miller, R.D., Park, C.B., and Tian, G., 2003, Inversion of high frequency surface waves with fundamental and higher modes: Journal of Applied Geophysics, 52(1), 45-57.

Xia, J., Chen, C., Li, P.H., and Lewis, M.J., 2004, Delineation of a collapse feature in a noisy environment using a multichannel surface wave technique: Geotechnique, 54(1), 17-27.

Xia, J., Xu, Y., Miller, R.D., and Chen, C., 2006a, Estimation of elastic moduli in a compressible Gibson half-space by inverting Rayleigh wave phase velocity: Surv. Geophys., 27(1), 1-17.

Xia, J., Xu, Y., Chen, C., Kaufmann, R.D., and Luo, Y., 2006b, Simple equations guide high-frequency surface-wave investigation techniques: Soil Dyn. Earthq. Eng., 26(5), 395-403.

Xia, J., Xu, Y., and Miller, R.D., 2007a, Generating image of dispersive energy by frequency decomposition and slant stacking: Pure and Applied Geophysics, 164(5), 941-956.

Xia, J., Nyquist, J.E., Xu, Y., Roth, M.J.S., and Miller, R.D., 2007b, Feasibility of detecting near-surface feature with Rayleigh-wave diffraction: Journal of Applied Geophysics, 62(3), 244-253.

Xia, J., Miller, R.D., and Xu, Y., 2008, Data-resolution matrix and model-resolution matrix for Rayleigh-wave inversion using a damped least-square method: Pure and Applied Geophysics, 165(7), 1227-1248.

Xia, J., Cakir, R., Miller, R.D., Zeng, C., and Luo, Y., 2009, Estimation of near-surface shear-wave velocity by inversion of Love waves: Technical Program with Biographies, SEG, 79th Annual Meeting, Houston, TX, 1390-1395.

Xia, J., Xu, Y., Miller, R.D., and Zeng, C., in press**,** A trade-off solution between model resolution and covariance in surface-wave inversion: Pure and Applied Geophysics.

Xu, Y., Xia, J., and Miller, R.D., 2006, Quantitative estimation of minimum offset for multichannel surface-wave survey with actively exciting source: J. Appl. Geophys., 59(2), 117-125.

Xu, Y., Xia, J., and Miller, R.D., 2007, Numerical investigation of implementation of air-earth boundary by acoustic-elastic boundary approach: Geophysics, 72(5), SM147-SM153.

Xu, Y., Xia, J., and Miller, R.D., 2009, Approximation to cutoffs of higher modes of Rayleigh waves for a layered earth model: Pure and Applied Geophysics, 166(3), 339-351.

Zeng, C., Xia, J., Liang, Q., and Chen, C., 2007, Comparative analysis on sensitivities of Love and Rayleigh waves: Technical Program with Biographies, SEG, 77th Annual Meeting, San Antonio, TX, 1138-1141.

Zhang, S., and Chan, L., 2003, Possible effects of misidentified mode number on Rayleigh wave inversion: Journal of Applied Geophysics, 53, 17-29.